



### D4.3 Identified privacy threats and counter measures

Grant Agreement Number	101099491
Action Acronym	HOLDEN
Action Title	Ethical Design of Holography with Dense wireless Networks (HOLDEN)
Funding Scheme	HORIZON-EIC-2022-PATHFINDEROPEN-01
Version date of the Annex I against which the assessment will be made	13/12/2022
Start date of the project	1/6/2023
Due date of the deliverable	31/05/2025
Actual date of submission	30/05/2025
Responsible	CNR
Contributors	CNR, TWE, POLIMI, AAL
Dissemination level	Public



## Authors in alphabetical order

Full Name	Organisation	E-mail
C. Aydin	TWE	c.aydin@utwente.nl
S. Cammers-Goodwin	TWE	s.i.cammers-goodwin@utwente.nl
M. D'Amico	POLIMI	michele.damico@polimi.it
T. Eidbert	TUM	eibert@tum.de
S. Kianoush	CNR	sanaz.kianoush@cnr.it
U. Milasheuski	CNR	usevaladmilasheuski@cnr.it
A. Paulus	TUM	a.paulus@tum.de
V. Rampa	CNR	vittorio.rampa@ieiit.cnr.it
D. Salami	AALTO	darius.h.salami@aalto.fi
S. Savazzi	CNR	stefano.savazzi@cnr.it
S. Sigg	AALTO	stephan.sigg@aalto.fi

## Change History

Version	Date	Status	Author (Company)	Description
1.0	20.03.2025	Initial	CNR	First version
2.0	27.03.2025	Revision	CNR	Second version
3.0	16.04.2025	Revision	TWE and ALL	Third version
4.0	13.05.2025	Revision (FINAL)	CNR	Final revision

## Executive Summary

The present deliverable identifies and studies the main threats in RF sensing of human bodies and possible technical counter-measurements and fundamental signal processing tools that can be used to limit such identified risks.

RF sensing analysed in the Holden project is an emerging technology paradigm to utilize electromagnetic signals scattered off objects or subjects for sensing. The technology repurposes existing wireless communication networks for imaging and computer vision applications, namely ambient human sensing. For cellular communication systems, this results in a ubiquitous sensing infrastructure, able to “photograph” an environment, connect stimuli to a larger local, national or global picture, and to track subjects seamlessly.

For the above reasons, the possible social and ethical implications may be surprising and drastic and are currently underexplored. The deliverable showcases promising research directions in this new field and lays the groundwork for ethically compliant technology design, highlighting the challenges and potential solutions that can stimulate new research.

The deliverable is organized as follows.

First, emerging solutions to enable RF holography in static and dynamic environment are briefly discussed as the results of the activities in WP2, WP3 and WP4, together with data processing and hardware design choices to enable privacy by design. A mixed-method ethical approach is then analyzed to address social, legal and ethical implications of the technology.

Next, the deliverable proposes and discusses three promising technical mitigation measures that are generally designed to limit the ability for unethical use of RF sensing technologies. These enablers target the problem of:

- 1) RF signal and propagation manipulation, namely the use of beamsteering and reconfigurable surfaces,
- 2) physics-driven generative machine learning (ML), discussed in D3.6, which limits personal data collection and acts as privacy filter for de-personalization,
- 3) selective obfuscation via machine unlearning techniques.

Initial examples for RF sensing are finally discussed focusing on crowd dynamics tracking application use cases. The key point we have highlighted is the trade-off between accuracy and ethical design, which is measured in terms of *statistical parity*. Increasing the number of antennas provides accuracy benefits in RF sensing, however a performance disparity is also observed. In other words, a trade-off exists between equality and accuracy; increasing equality may decrease accuracy.

The following contents are also covered:

- A short introduction of the HOLDEN project and the collaboration partners.
- A theoretical background of RF sensing systems leveraging WiFi signals to track body motions in dynamic environments and their possible privacy threads targeting human body sensing.

- Description of three technical mitigation measures, namely in the form of signal processing-level technology means, to limit the unethical use of the RF sensing technology
- The proposed enabling technologies is then qualitatively and quantitatively verified in terms of feasibility and through examples.
- Finally, the deliverable proposes some quantitative metrics to assess equality in RF sensing. These metrics are evaluated targeting the problem of passive localization and counting of the number of subjects co-present (infrastructural snapshot of the environment)

# Table of Contents

<b>Abbreviations</b>	<b>6</b>
<b>1. Introduction</b>	<b>7</b>
1.1. About HOLDEN	7
1.2. Partners	7
<b>2. Ethical design in RF sensing</b>	<b>9</b>
<b>2. RF holography: main threats in human sensing</b>	<b>11</b>
2.1. Holographic body scanning	11
2.2. People analytics through WiFi signals	13
2.3. Gesture and pose recognition	13
2.4. Preventing malicious algorithm behavior	14
<b>3. Counter measures and technical enablers</b>	<b>15</b>
3.1. Smart and reconfigurable radio environments	15
3.2. Physics-informed generative machine learning	17
3.3. Ethical scalability: obfuscation and unlearning	18
<b>4. RIS aided localization in a confined space</b>	<b>19</b>
<b>5. Main ethics measures for RF sensing</b>	<b>22</b>
<b>6. Case study examples</b>	<b>23</b>
6.1. Scenario and graph neural network model description	24
6.2. Multi-target discrimination: accuracy results	25
6.3. Multi-target discrimination: statistical parity	27
<b>7. Conclusions</b>	<b>30</b>
<b>3. References</b>	<b>31</b>
<b>9. List of figures</b>	<b>33</b>

# Abbreviations

---

Abbreviation	Description
3D	three-Dimensional
Aalto	Aalto University
BPA	Back Projection Algorithm
CNR	Consiglio Nazionale delle Ricerche
EC	European Commission
EM	ElectroMagnetic
EU	European Union
FEM	Finite Element Method
GTD	Geometrical Theory of Diffraction
HE	Horizon Europe
HOLDEN	Ethical design of holography in dense wireless networks
MIMO	Multiple Input Multiple Output
MoM	Method of Moments
NN	Neural Network
PEC	Perfect Electric Conductor
RF	Radio Frequency
TUM	Technical University of Munich
TWE	University of Twente
UTD	Uniform geometrical Theory of Diffraction
WP	Work Package
CSI	Channel State Information
CQI	Channel Quality Information
MUSIC	MULTiple Signal Classification

# 1. Introduction

---

## 1.1. About HOLDEN

The ubiquitous perception by sensing of objects, subjects, and gestures is a pivotal challenge for future technology: it enables personalized services such as smart living, automated logistics, or interaction through free-space gestures. However, it also challenges ethical and moral boundaries, and threatens privacy. HOLDEN proposes a radically new approach to RF-based perception by concisely analysing ethical constraints and privacy risks while re-thinking RF-based sensing. We establish necessary conditions for privacy preserving and ethically compliant sensing, and develop new paradigms respecting these constraints.

For the first time ever, HOLDEN constitutes a concentrated effort to explore social aspects of RF-sensing to guide the technological advance, and to derive technology for ethically and privacy compliant perception. The development of ethical and privacy constraints is central to HOLDEN. We use these findings to derive privacy- and ethically-compliant concepts for RF-based perception. We will develop a system of distributed multi-antenna devices for simultaneous multitarget recognition and ubiquitous perception with unprecedented accuracy, which constitutes a radical paradigm shift from a technology-centric perspective to a privacy-centric one via a privacy-by-design approach.

HOLDEN achieves this goal along three high risk, complementary, and privacy-centric paths:

Path 1: Continuous-space measurement points: Radio-based 3D vision by holographic image processing of RF wavefronts.

Path 2: Discrete-space measurement points: Advanced 3D beamforming for human-scale recognition and tracking through dense, massive, and connected antenna arrays.

Path 3: Signal processing and learning: High-dimensional tensor processing for the distinction of complex activities and motion from massive-dimensional RF data. The resulting breakthrough approaches and algorithms will be compared against application-level benchmarks via usage scenarios in the fields of logistics, smart living, and free-space.

## 1.2. Partners

The consortium consists of four academic partners and a high-tech SME partner: (a) Aalto University (AALTO), Finland, (b) Technical University of Munich (TUM), Germany, (c) Consiglio Nazionale Ricerche (CNR), with third party Politecnico di Milano (POLIMI), Italy, (d) University of Twente (TWE), Netherlands, and (e) Adant (Adant), Italy. This consortium features the specialized and complementary expertise required to achieve the project objectives. AALTO will be responsible for the project management (WP1), covered by an experienced and dedicated project manager. Ethical aspects (WP2) will be addressed by TWE (Prof. Ciano Aydin) who is a pioneer in the field. Eventual gender differences in the ethical perception will be considered. TUM pioneered RF holography, which makes TUM (Prof. Thomas Eibert) the ideal leader of WP3. In advanced

distributed signal and information processing, CNR has through Prof. Stefano Savazzi more than 14 years of experience. CNR will lead WP4. Since more than 10 years, AALTO is active in radio sensing and machine learning based activity recognition. This expertise makes AALTO (Prof. Sigg) the ideal leader of WP5. Adant (Daniele Piazza) will contribute to the market analysis, application possibilities, and validation (WP6). Led by AALTO, dissemination with the website as one the media will be addressed by all partners. All academic partners are committed to early publication of results, e.g., via arXiv (open science).

## 2. Ethical design in RF sensing

---

RF holography can transform wireless communication networks into radio sensors that allow the mapping of objects as well as human-scale sensing. Stray fields emitted from wireless devices are recorded in a phase-sensitive manner and visualized in 3D to reconstruct or map the surrounding environment [1].

Such ubiquitous perception through RF signals is a pivotal opportunity for future technology: it enables personalized services such as smart living, remote healthcare, automated logistics or interaction through free-space gestures [3]. The ubiquity of Wi-Fi and cellular networks presents a powerful platform for the development of innovative holographic tools. Future standards will also introduce dedicated sensing features which will allow routers to work as radar devices [4].

With increasing frequency, bandwidth and antenna count, novel RF sensing solutions may soon reach comparable quality as classical vision approaches and even surpass vision-based techniques. Interpreting stray radiation from ubiquitous wireless devices, as shown in Figure 1, might target the reconstruction of 3D environments to resolve objects or individuals inside crowds [5]-[10] and under variable environmental conditions, i.e., dark or occluded spaces, and non-Line-of-Sight (NLOS).

On the other hand, integrating RF holography into ubiquitous communication systems may have unforeseen social and ethical consequences, both positive and negative. In this deliverable, we identified such implications and target the design of ethically compliant RF holography methods by focusing on several technical countermeasures. To limit possible negative outcomes, novel research directions consider design paradigms that may constrain system capabilities, such as limiting the sensing range, obfuscation of unauthorized areas and enforcing the individual's right to be excluded (or be forgotten) by the sensing system.

The need for novel "ethically scalable" RF sensing tools is expected to emerge soon, since the technology is evolving and already integrated in various forms in research and patents. Future development of the technology therefore demands an effort to embed ethics into the design and application of what may soon be an enabling technology – a technology that provides the basis and support for other systems.

In the present Deliverable D4.3 we explore challenges and opportunities of ethics-by-design in RF sensing, examining recent research and technological advancements in the field. The deliverable identifies first the possible ethical and privacy threats focusing specifically on dynamic tracking of body movements, as the focus on WP4, next we discuss the main technical counter measures, namely specific technology means to limit the unethical use of the technology as well as improve its performance in real environments. Design models, technical and ethics measures are discussed, exploring their potential role in future regulatory efforts.

**Subject A** (demographic group A)   **Subject B** (demographic group B)  
**Area A** (unprivileged or authorized)   **Area B** (privileged or unauthorized)

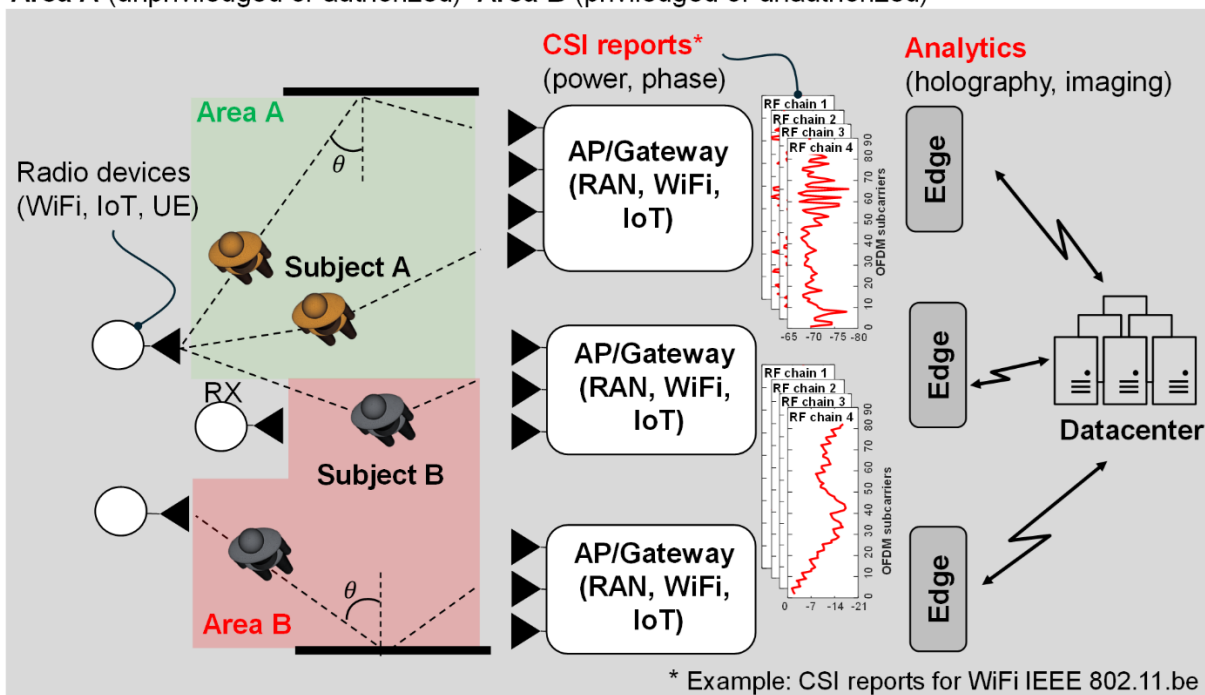


Figure 1: RF holography system to repurpose communication networks: architecture example, CSI reports and analytics

## 2. RF holography: main threats in human sensing

---

RF sensing and imaging technologies utilize discrete samples of the electromagnetic (EM) fields, channel state information (CSI) measurements or spatially consistent transmission/scattering data obtained in confined measurement areas, such as home, buildings, and open spaces. They generally aim to reconstruct the shape, size, material properties, and relative location of unknown scattering objects in the environment.

Due to its non-ionizing nature and ability to penetrate dielectric materials, microwave imaging tools have been extensively studied over the past few decades [1]. Imaging algorithms are often based on the concept of tomography and holography by passive synthetic aperture radar (SAR): they use ubiquitous EM waves as imaging sources, such as Wi-Fi, cellular or short-range radio signals, without the need for a dedicated transmitter.

In static imaging, addressed in WP3, the goal is to visually “photograph” static target(s) or object(s) of interest in 2D or 3D. In contrast, dynamic RF sensing [3], addressed in WP4, focuses on the detection and tracking of object(s) or human body motions. The terms “static” and “dynamic” here refer to data acquisition processes which are either much slower (“static”) or much faster (“dynamic”) than changes of the scenario to be investigated. Deploying RF sensing in dynamic environments requires careful consideration of practical constraints, including limited antennas, carriers, and sampling times. These limitations often coexist with advancements in Wi-Fi technology. In what follows and through the present deliverable, we will focus primarily on dynamic RF sensing as the target of WP4

### 2.1. Holographic body scanning

The idea of holographic imaging is to illuminate a region of interest with EM waves and to record the superposition of the incident and scattered field within a sufficiently large area with a measurement device. The overall size of this measurement area, the number of samples acquired, the frequency range used, as well as the diversity of the illumination strongly affect the achievable image quality. Under the assumption that no objects within the region of interest move during the period of the measurement (“static”), and with a suitable choice of these parameters, accurate three-dimensional recordings of arrangements and geometries can be generated.

A typical holographic measurement application is depicted in Figure 2, where simulation and measurement results are shown on the bottom left and right, respectively. In both cases, a single fixed transmitter is utilized to illuminate a human phantom, and the scattered field is recorded on a planar surface at less than 2m. Image generation is then performed on a computer utilizing phase and magnitude data at multiple frequencies. In real-world measurements, the required phase information can for example be obtained via a reference antenna. The resulting images shown in Figure 2 are projections of the obtained three-dimensional scattering distributions to the frontal cross-section of the region of interest. In general, the achievable image quality depends on the illumination of the scenery, the scattering behavior of the illuminated objects and on the spatial

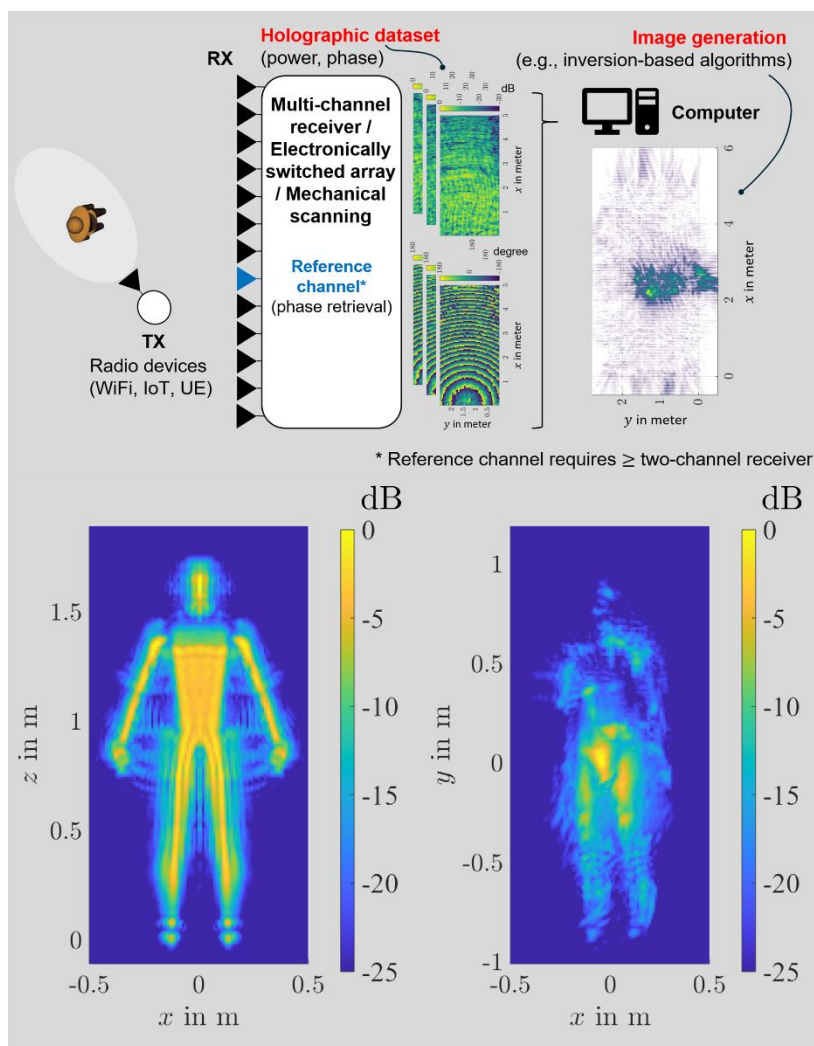


Figure 2: Holographic imaging: body scanning concept for a human phantom

distribution of the observations. An incomplete image (Figure 2 bottom right) may result if the illumination is not properly chosen. For the results, signals between 6 GHz to 8 GHz were used in the simulation, and a frequency range of 6 GHz to 12 GHz was utilized in the measurements. Larger bandwidths lead to a better depth resolution, i.e., perpendicular to the measurement surface, while larger frequencies allow to resolve fine details of the scenery. Lower frequencies can help to look inside of or through objects and tend to cause a more even illumination of the region of interest.

With the ever-increasing bandwidth and frequencies utilized by future Wi-Fi systems, purely passive holographic imaging could potentially be a key technology for the advancement of smart systems, e.g., smart homes and cities. On one hand, technological challenges, i.e., recording thousands of measurement samples on surfaces of multiple square-meter within milliseconds, will need to be solved before indoor holographic imaging of living beings ("dynamic") with Wi-Fi signals comes into reach. On the other hand, it is already foreseeable that the anticipated image quality will enable indirect identification and differentiation of individuals, for example, based on body size and shape.

Given the ubiquity of Wi-Fi today, a discussion about the ethical consequences and societal impact of RF holography should not be deferred to the future. While technology is still being developed, it is also more feasible to make adjustments to its design based on the results of these considerations.

## **2.2. People analytics through WiFi signals**

As 6G and beyond technologies are still emerging, Wi-Fi has quietly become a ubiquitous presence in millions of homes, supported by major internet service providers, smart-home companies, and chip manufacturers. This widespread availability makes Wi-Fi an appealing platform for developing innovative holography tools, especially as network performance continues to improve. Most of the current chip designs support ad-hoc firmware for CSI measurement report extraction with multiple-input multiple-output (MIMO) arrangements of the transmitter (TX) and receiver (RX) antennas and Orthogonal Frequency Division Multiplexing (OFDM) subcarriers. However, much still needs to be done to make RF holography suitable for implementation in these chipsets. Beyond the need for dense measurements and antenna deployments in confined areas, accurate and computationally efficient physical models [10] are also required to predict the human body blockage, namely the effects of body motions on CSI.

CSI hologram tensor structures provide a full representation of RF radiation observed over consecutive time symbols, subcarriers and antennas (RF chains). As depicted in Figure 1, the CSI describes the phase shift and amplitude of multiple propagation paths on each subcarrier. Advanced Wi-Fi systems powered by beam-switching capabilities also allow the antenna radiation beams to be controlled in real time, thus offering additional degrees of freedom for sensing.

The latest standards, IEEE 802.11ax and IEEE 802.11be (WiFi 7) standards introduced an additional 6GHz carrier option, expanding upon the traditional sub-7GHz carriers (2.4GHz and 5GHz). Moreover, as highlighted in previous deliverable Wi-Fi 7 offers a wider subcarrier bandwidth of 160MHz (up to 320MHz), providing at least 120 usable pilot subcarriers for CSI or Channel Impulse Response (CIR) estimation. Future standards will lead to another leap in CSI analysis [4] by introducing advanced CSI acquisition modes, as well as the possibility of estimating the channel state for non-associated neighboring devices.

Wi-Fi signals could be exploited to track daily human movements and behaviors, potentially leading to both beneficial and harmful, as well as unexpected ends. For example, Wi-Fi signal variations have been shown to differ between individuals [5] and can consequently be used for re-identification. Crowd sensing and counting systems that interpret smartphone Wi-Fi signals have been deployed in large public areas [7] with performance comparable to classical vision systems. The ownership of this information, its intended use, and its impact on human interaction hold significant social and ethical implications.

## **2.3. Gesture and pose recognition**

In view of the steady increase of the performance and capabilities of Wireless Local Area Networks (WLANs), the IEEE 802.11bf standard [4] will introduce dedicated sensing features that heavily rely

on sophisticated hardware and which, for example, will allow routers to work as frequency modulated continuous wave radio detection and ranging (radar) devices targeting also mm-wave frequency bands to even 60 GHz.

Independent of standardization, there are already products offering Wi-Fi embedded sensing, such as Intel's Wi-Fi Proximity Sensing, Cognitive (cognitivesystems.com) and Origin (originwirelessai.com) systems. CSI tensor analytics often use point cloud data representations similar to radars, which enable efficient spatial filtering options to improve scalability as well as contribute to privacy. Several radar designs have been successfully deployed and installed targeting precise half and full body gesture, pose and activity recognition [8][9]. These studies demonstrate the feasibility of achieving high gesture recognition accuracy, with reported accuracies ranging from 66% to 98% for complex gesture sets. Despite these promising results, ensuring robust performance can conflict with minimizing data collection and protecting individual privacy: balancing functionality and privacy remains a key challenge in next generation sensing systems.

## **2.4. Preventing malicious algorithm behavior**

Machine learning (ML) and AI tools play a pivotal role in RF sensing and holography. A variety of datasets [11] representing diverse environments, people, RF hardware and networks are also readily available for ML research purposes. While infusing ML algorithms with human-like morality or values is currently unfeasible (known as the value alignment problem), recent efforts have focused on developing proactive mechanisms to prevent undesirable behavior through probabilistic safety guarantees (Seldonian framework [12]), as well as reactive methods which unlearn pre-trained functions or specific data [13].

As considered in the following, a complementary approach to algorithmic solutions involves the proactive design of RF environments, where signal propagation and training data are carefully controlled to mitigate potential undesirable behaviors.

### 3. Counter measures and technical enablers

The development of technological solutions (or countermeasures) with ethical scalability in mind is discussed in the following section. Three key technology enablers are proposed as mitigation measures to limit the ability for unethical use of the RF sensing technologies, namely to prevent sensing algorithms to identify individuals or monitor spaces any more than is necessary for the functioning of the technology. These countermeasures are described in the following section.

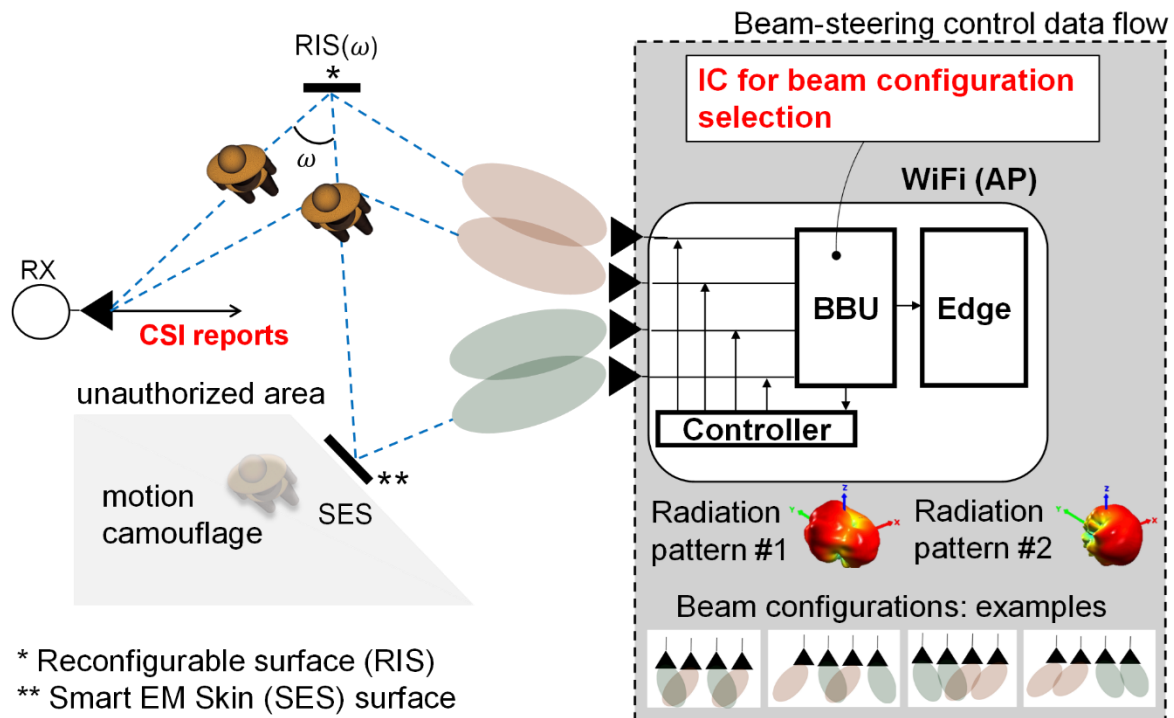


Figure 3: Smart and reconfigurable radio environment example: beam-switched system integrated with WiFi setups, reconfigurable and smart skin antenna surfaces

#### 3.1. Smart and reconfigurable radio environments

The first technical enabler concerns the manipulation of the RF signals or the radio propagation: realizing a purpose-built EM environment is of paramount importance to implement scalable sensing. Two technologies are under exploration. The first one is beam steering, which is useful to increase the sensing performance in specific spots/locations/monitored areas. Second, the use of RF signals at high frequency, from mmWave and subTHz [8], to improve the resolution and reduce the sensing range, for example sensing in NLOS which might cause privacy leakage.

Sensing and imaging operations may require customized approaches depending on the specific area being monitored. For example, some “privileged” areas or with limited access might need to be obfuscated or camouflaged as they require more privacy guarantees than “unprivileged” or authorized ones. In what follows, we discuss two popular communication technologies designed

for the manipulation of the radio environment, which are repurposed here for ethically scalable RF sensing.

As depicted in the example of Figure 3, smart reconfigurable antennas offer the ability to dynamically shape radiation patterns, directing energy towards desired spots. This capability is essential for both 6G and next-generation Wi-Fi systems, while it has been recently re-designed as a new opportunity for human-scale passive RF sensing [10]. Reconfigurable antennas are quite different from antenna arrays since they do not require precise phase alignment. Also, unlike beam-forming, the radiation patterns can be dynamically altered on each antenna separately by changing the current distribution on each of the radiating elements. In addition to enabling scalable sensing, beam-steerable antennas can be effectively repurposed to mask body movements in specific unauthorized spots, making the technology adaptable to various regulatorily pre-imposed constraints or challenges that stem from stakeholder needs.

Reconfigurable Surfaces (RIS), or EM Skins (EMS), can also serve as effective solutions for manipulating the propagation of signals and produce a purpose-built radio environment to satisfy specific sensing constraints. While RIS surfaces provide near real-time adaptability, as they can macroscopically behave as a steerable mirror that reflects the impinging signal towards a desired direction ( $\omega$ ), EM skins can help optimize RF environments during the pre-deployment design phase, to minimize unintended signal propagation and mask body movements in specific areas. The coordinated use of RIS and EMS technologies to control the radio environment is an open research area.

We refer to Sect. 5 for a more specific description of an example scenario and results on the topic.

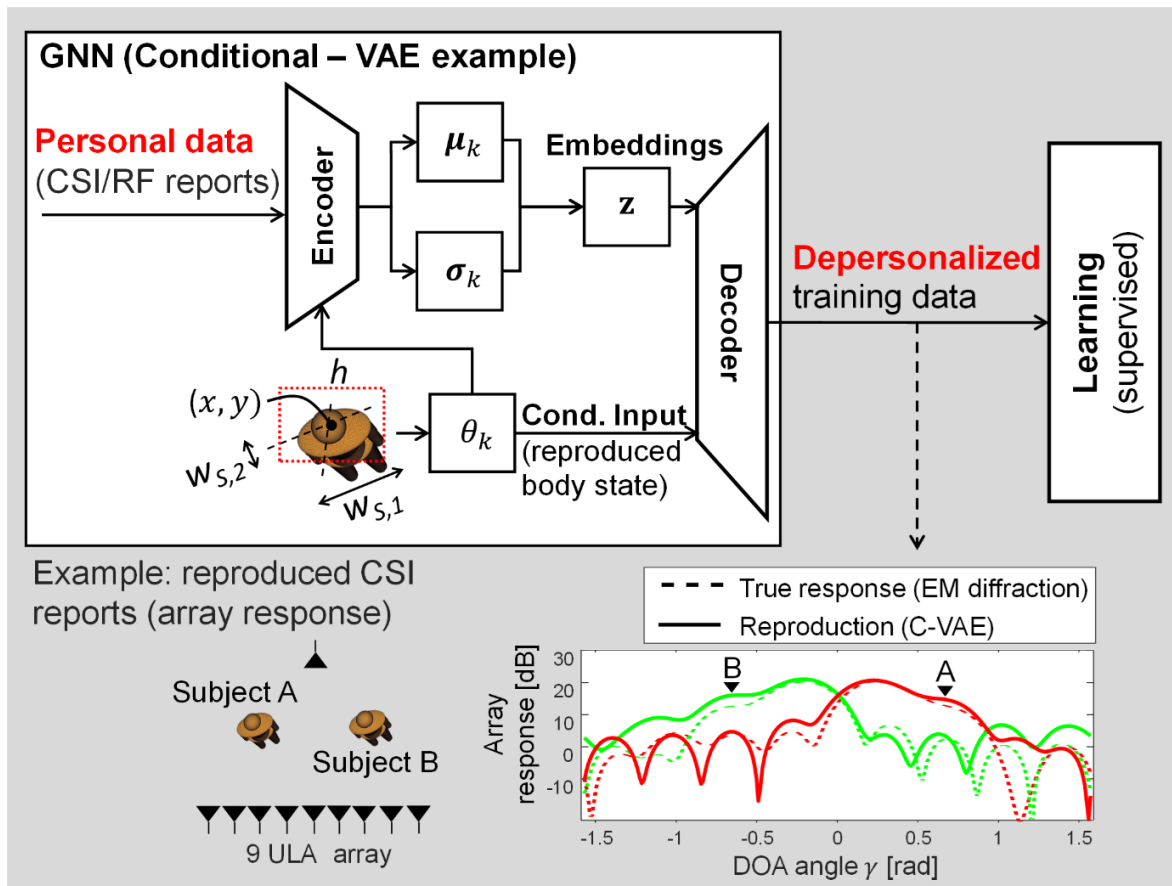


Figure 4: Physics-driven generative machine learning example for reproduction of the array response from a ULA of 9 antennas. Ethical filtering for depersonalized training data

### 3.2. Physics-informed generative machine learning

Physics-informed generative models use AI and ML for computing physical processes. They aim to learn and reproduce observations that reflect the physics underlying the radio propagation [15]. Early attempts to generate synthetic CSI reports to reproduce the effects of human motions on the RF field have relied on generative deep neural networks (GNNs). Popular techniques such as Generative Adversarial Networks (GAN), diffusion models, and conditional Variational Autoencoders (C-VAE), [10] have been shown to limit the use of time-consuming EM computations. Vision and Large language models [15] repurposed for the task have also demonstrated effectiveness in generating massive MIMO CSI structures.

Figure 4 shows an example of C-VAE based reproduction of the CSI reports obtained from a RX receiver equipped with 9 antennas and a single antenna Wi-Fi transmitter at 2.4GHz. Reproduced CSI are used to obtain the array beamforming response as function of the direction of arrival (DoA). In the example, we consider a subject located at two distinct nominal displacements from the LOS (namely A and B). The figure represents the effects of a target, as moving from location A to location B, on the beamforming response. The goal is thus to highlight how array responses are affected by the specific body location. Please refer to deliverable D3.6 for a more complete description of the scenario/tests. In general, the generated responses (solid lines) well replicate diffraction effects

(dashed lines), yet without the need of collecting biometric data or personal information. For example, it can be noticed that the maximum response of the array (see triangle markers) is perturbed by the presence of the subject and such alteration is well reproduced by the C-VAE generative model.

While still in their infancy, we expect GNNs to effectively serve as “ethical filters” capable of generating depersonalized training data from a synthetic environment, to mitigate the risk of malicious use, bias or person (re)identification. GNNs thus hold the potential to enhance the transparency and scalability of RF sensing as well as its training data handling practices.

### **3.3. Ethical scalability: obfuscation and unlearning**

Ethically and privacy scalable RF sensing demands the ability to selectively unlearn functions that could potentially facilitate unethical use or unintended consequences. This adaptability allows the trained AI or machine learning model to evolve in response to changing ethical profiles and constraints. Machine *unlearning* refers to the process of selectively removing training data and their influence on a pre-trained model, making the updated model behave as if it was never trained on that data [13]. Being initially proposed to address 'Right to be Forgotten' regulations in what follows, we explore the tool as an additional foundational technology for ethically scalable RF sensing.

An unlearning mechanism could enable the selective removal of specific user information from the RF sensing model, while retaining critical task features. An example is provided in [8] [9] where an attempt was made to train the RF sensing model to maximize accuracy while simultaneously reducing user identification performance. Validation on RF signal-based gesture recognition datasets [8] [9], demonstrates the framework effectiveness, achieving high gesture recognition accuracy while significantly reducing user identification capabilities. Further analysis will be carried out in WP5.

On the Pantomime dataset [8], gesture recognition accuracy decreased from 98% to 90%, while user recognition accuracy dropped significantly from 70% to 9%. Similarly, on the mHomeGes dataset [9], gesture recognition accuracy decreased from 88% to 83%, and user recognition accuracy dropped from 66% to 20%. These results highlight the potential of this approach in balancing functionality and privacy in next-generation RF sensing applications.

## 4. RIS aided localization in a confined space

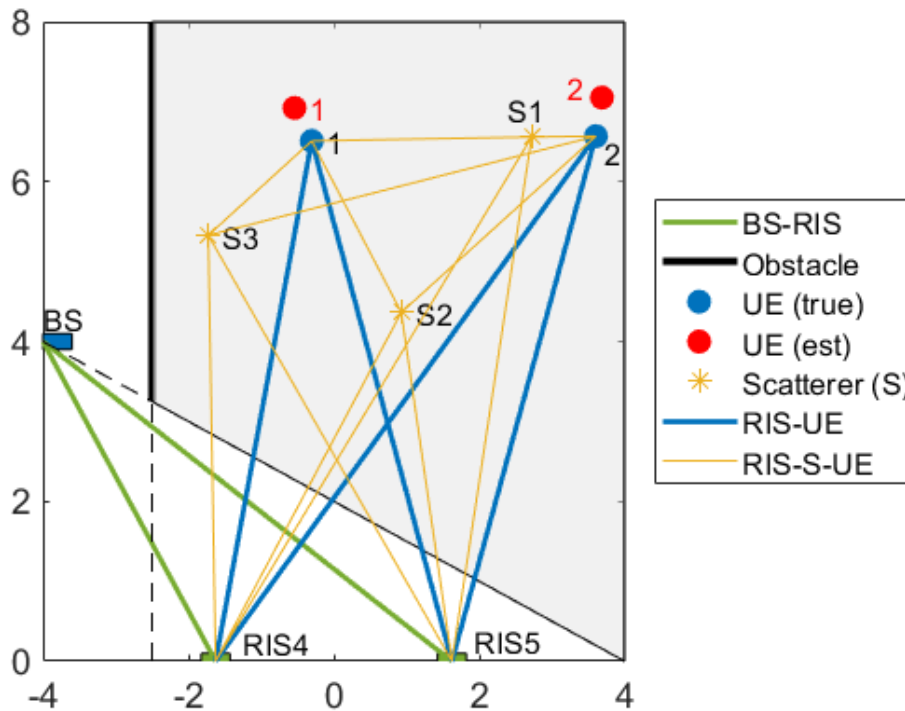


Figure 5: Localization of mobile device (UEs) inside a confined region using active RIS components: the smart radio environment is simulated for communication performance assessment: two UE are moving randomly in the monitored area and communicating with the BS.

In this section we discuss a novel approach which targets the integrated sensing and communication in an indoor smart radio environment (shown in Figure 5) where the LoS links between mobile devices (UE) and the AP (or Base Station – BS) are blocked by an obstacle. Several RISs are deployed to establish virtual LoS UE–BS links and provide a localization service inside the authorized area (area shaded in grey in the Figure) which is not covered by the AP.

The design parameter of each deployed RIS is its electronic steering angle (or electronic rotation  $R$ ). A RIS, electronically adjusted by a specific rotation behaves like an anomalous mirror that appears to be rotated by an angle. This process is typically automated and controlled through sophisticated algorithms. At any given time, the RIS-aided smart radio environment (see Figure 5) can be dynamically configured by optimizing the vector of RIS rotation angle, thereby maximizing performance metrics such as the overall network throughput or the received signal strength.

In the considered example of Figure 7, we want to verify how RIS surfaces can enable the RF sensing system to effectively monitor the area not covered by the BS. Targeting integrated localization and communication services, we also implemented [17] a time resource allocation strategy aiming to achieve the best compromise between UE positioning accuracy in the considered area and throughput.

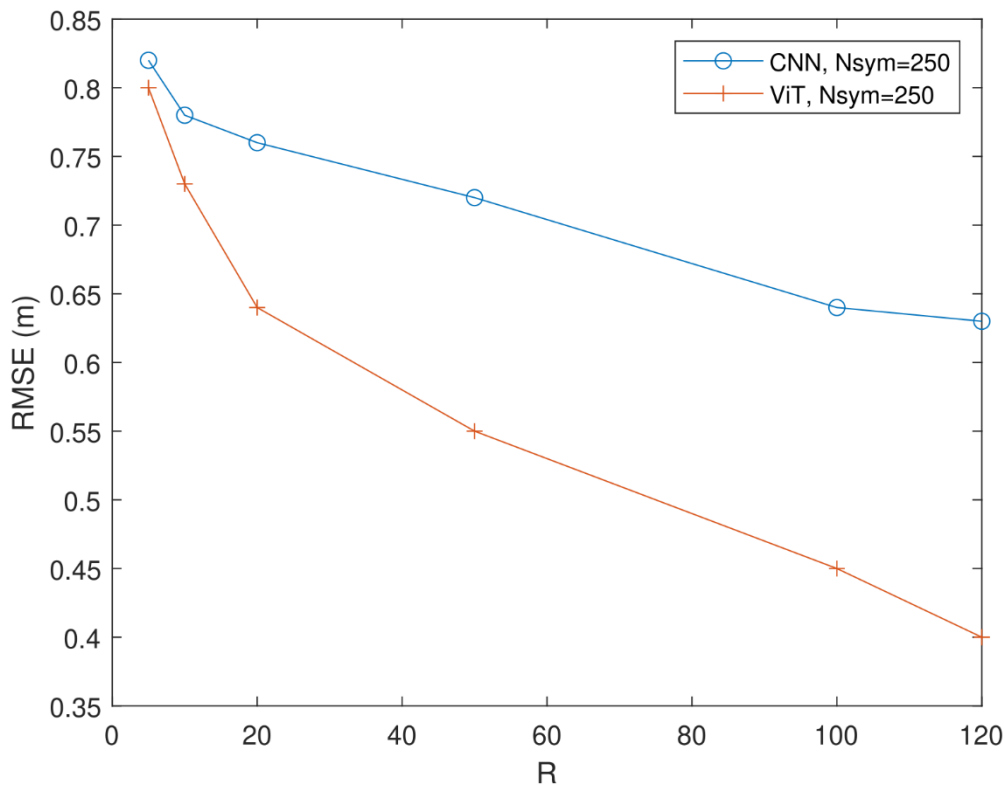


Figure 6: Root Mean Square Error (RMSE) result of UE localization Using CNN and vision transformers (ViT) for the same scenario presented in figure 7. The RMSE result for  $N_{sym}=250$  (i.e., simulated samples) and for varying number of RIS electronic rotations  $R$ .

The process went through the following key steps:

1. The Cramer-Rao lower bound to positioning accuracy was evaluated and verified as a tool for pre-deployment assessment of RIS in indoor environment. For the considered scenario, we concluded that three RIS are sufficient for providing a good localization performance in the area not covered by the AP.
2. Localization of devices was implemented by exploiting (i) the above set of RIS, acting as electronically steerable reflectors, used to scan the environment where the devices are located and (ii) two different localization algorithms based on Convolutional Neural Network (CNN) and Vision Transformer (ViT) DL models. The performance of both algorithms was tested and verified as shown in Figure 6.
3. We evaluated the performance of both deep learning algorithms (CNN and ViT) in terms of RMSE for varying number of RIS rotations  $R$ , considering also two different computational capabilities of the BS equipment, namely a low-power (IoT) and a high performance (HPC) device. The simulations showed that, while a longer localization time ensures a smaller positioning error, there is no apparent benefit in reducing the localization error below 0.6 m as this would subtract re-sources useful for communication, decreasing the frame efficiency and the network throughput.

4. An optimal tradeoff exists between frame efficiency and localization accuracy, leading to a maximum of the network throughput. The above optimum corresponds to frame efficiency values between 0.75 and 0.98, depending on the computational capability of the devices as well as on the localization algorithm. It turns out that the low-cost solution featuring CNNs operated over IoT devices provides a slightly higher throughput than ViTs operated over HPC hardware.

## 5. Main ethics measures for RF sensing

---

In this section we consider the configurable elements of the technology, as introduced previously, and how to ethically optimize their impact. We thus examine selected quantitative ethics metrics [15] and provide an example of how these can be used to identify and quantify ethical issues in a selected RF sensing pipeline.

Existing metrics considered in the following predominantly address equality and uncertainty quantification, namely they quantify potential biases related to human body physical attributes, locations, and activities as well the reliability of the AI model outputs.

1. *Statistical parity* (demographic parity or statistical distance) Measures the difference between the probability of a prediction being positive between two different groups. In RF sensing, groups are differentiated by unique EM characteristics associated with specific physical body attributes (i.e., size, behavior, pose). The main goal is to penalize model predictions that are biased with respect to specific human body attributes.
2. *Equalized odds* ensure equal prediction accuracy across different groups. Different from parity, the metric penalizes models that exhibit strong performance solely on the majority of the groups. Notice that any discrepancy should be publicized via rigorous uncertainty quantification, so that users are aware, and the technology is not misused for the minority of people for which it will not work for. For example, recognition of subjects or gestures should be comparable across different human bodies.
3. *Predictive equality* measures the accuracy balance by false positive rates (FPR). This metric is applicable in contexts where the monitored area is segmented into privileged and non-privileged zones (see Figure 1). As discussed in the previous example, it is crucial to ensure “equal obfuscation” for all subjects moving, or performing gestures, inside areas where the subjects do not agree to be tracked (or where detection is not allowed).
4. *Expected Calibration Error* (ECE) Rigorous uncertainty quantification in ML model outputs should be carefully considered to guarantee the reliability of results. The performance metric chosen for assessing the reliability is the widely adopted Expected Calibration Error (ECE) [22][24]. This metric quantifies the mismatch between the accuracy and the confidence of the model.

An example is now provided to show the application of *statistical parity*, in conjunction with *accuracy*, for ethical evaluation of a RF sensing pipeline.

## 6. Case study examples

We now consider a dense deployment of wireless communication radio devices (i.e., nodes) collecting RF measurements from which to reconstruct an “infrastructural snapshot” of the environment [16]. As depicted in Figure 7 the goal is to obtain an accurate prediction of the number of subjects (i.e., the targets) moving in the considered space as well as to capture the body motion patterns on a given time instant  $t$ , by utilizing the same wireless communication services that they provide. Such an imaging of the scenario may be used to build a digital twin of the environment able to identify emerging or repetitive patterns of body movements with relevant applications in the field of smart spaces and assisted living.

We assume a multi-target scenario, where  $N > 1$  targets are moving randomly in the monitored area. Targets may freely enter or leave this environment as well. Therefore, the number of targets is considered as time-varying, namely  $N = N(t)$ . These  $N$  targets are characterized by different physical characteristics represented by an ensemble of features, namely the target location, its relative orientation the height  $h$ , and traversal size, namely the lateral and anteroposterior dimensions  $w_{S,1}, w_{S,2}$ .

In what follows, we analyze both the accuracy observed when counting the number of people present as well as the ability of the AI model (described in the following) to produce fair results, i.e. that they have no bias and behave in the same way depending on the characteristics of the monitored subject. We thus collect and report the *accuracy* and the *statistical parity* metric (Section 6) results for each considered scenario.

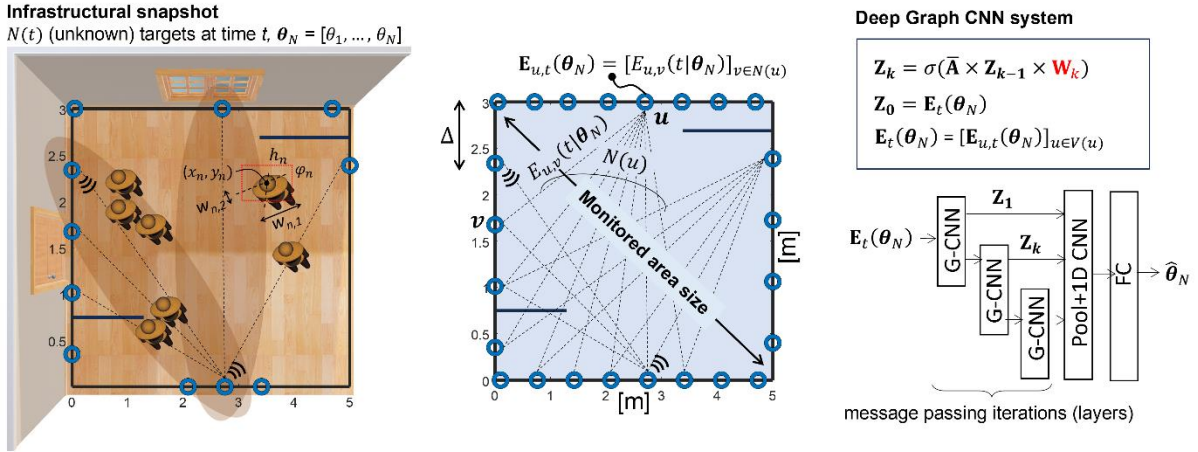


Figure 7: Infrastructure snapshot scenario: multi-target body counting through RF signals inspection. EM simulation environment, main parameters, network structure and DGCNN model approach.



Figure 8: Infrastructure snapshot scenario: deployment and tests in an indoor environment. Results will be discussed in WP6

## 6.1. Scenario and graph neural network model description

RF signals and EM field samples are organized into graph structures with nodes and edges corresponding to the antennas of the radio devices and the active communication links, respectively. This choice is motivated by node-invariant properties (i.e., permutation invariance) of RF sensing as applied to dense networks. The nodes of the graph collect high-dimensional features

represented here as the Channel State Information (CSI) obtained from signals overheard from 1-hop neighbours at time  $t$ . Features thus carry information about the presence of concurrently moving bodies/targets inside the 1-hop neighbourhood of the considered node. Considering the ensemble of nodes, every graph structure conveys an infrastructural snapshot of the environment at a specific time instant  $t$ . The problem we tackle is thus to track the number of targets  $N(t)$  concurrently moving in the space using unseen graph observations at any time  $t$ .

The problem of multi-target detection is formulated here as a classical graph classification problem [19][20]. The presence of targets modifies the RF field and gives rise to different populations of graphs and node features which encode information about the targets as well as their physical characteristics (i.e., locations, size, and motions). In the following we proposed a flexible classification tool based on Deep Graph Convolutional Neural Network (DGCNN) model which is trained using generated EM body model samples based on diffraction models (D3.6). The approach followed is thus to incorporate prior EM-model based knowledge into DGCNN neural architecture rather than resorting to supervised training which might suffer from overfitting.

## 6.2. Multi-target discrimination: accuracy results

Figure 7 considers a dense deployment of wireless radio devices collecting CSI data (we consider both 2.4GHz and 5.8GHz frequencies). We want to obtain a precise prediction of the number of subjects moving in the considered space (10x10m area) in each time instant  $t$ . A deep graph convolutional neural network (DCGNN) model is trained on synthetic data generated by C-VAE reproducing EM diffraction effects. Accuracy and statistical parity are evaluated for varying number of people ( $N$ ) co-present and featuring different physical characteristics (subjects A, B and C) reported in the caption. These physical characteristics refer to the EM body model that has been presented and discussed in the D3.6. Notice that the physical dimensions and crowd size significantly influence body diffraction effects and thus the RF sensing performance.

The Figure 8 presents a corresponding experimental deployment of the network nodes. The network architecture employs devices operating in the 2.4GHz frequency band and adhering to the IEEE 802.15.4 physical layer specification, a standard commonly adopted in industrial deployments. Further analysis of the results under this configuration will be carried out in WP6 and according to the identified performance metrics of WP5 and WP6.

Figure 9 and the table of Figure 10 report the complete counting accuracy analysis now considering

- 1) varying area size ranging from 10m x 10m (100 sqm) to 5m x 5m (25 sqm),
- 2) CSI collected at carrier frequencies 2.4GHz and 5.8 GHz (typical in WiFi settings).
- 3) Subjects A, B and C characterized by different physical characteristics (height  $h$ , lateral and anteroposterior dimensions  $w_{S,1}, w_{S,2}$ ).

For each considered case, the accuracy is obtained for varying number of antennas deployed, namely 25 and 60 antennas for 10m x 10m area, 20 and 60 antennas for 5m x 5m and 7m x 7m areas.

Figure 9 shows the accuracy in predicting the number of targets co-present within a 10m square area (100 sqm). Specifically, it compares subjects with different physical characteristics (A, B, C) in blue, red, and green, across various network topologies. In the example, three cases are highlighted: the first one aims to discriminate  $N=6$  subjects, the second  $N=10$ , and the third  $N=14$ . The density (spacing) of the deployed antennas (or nodes) significantly affects the performance: accuracy improves as antenna spacing decreases (and therefore as the number of antennas installed along the room's perimeter increases).

The table in Figure 10 reports all considered cases and accuracies as the number of detected targets increases from  $N=3$  up to  $N=20$ , along with frequency, from 2.4GHz to 5.8 GHz and room size. From the results in the table, the following conclusion can be made:

- 1) by setting a minimum accuracy of 70%, 60 antennas are generally needed to effectively discriminate up to  $N=14$  targets when room dimensions are greater than 7m (50-100 sqm).
- 2) up to  $N=10$  targets are detectable with accuracy above 70% in smaller areas (5m, 25 sqm) which is reasonable considered the space constraints.
- 3) subjects characterized by limited physical dimensions (e.g., target C) tend to be more difficult to detect due to diffraction effects, inequality/bias in detection should be therefore considered (see the following analysis).

The above results, based on simulations of CSI obtained from the multi-body EM diffraction model considered in D3.6, will be verified within the test house in WP6

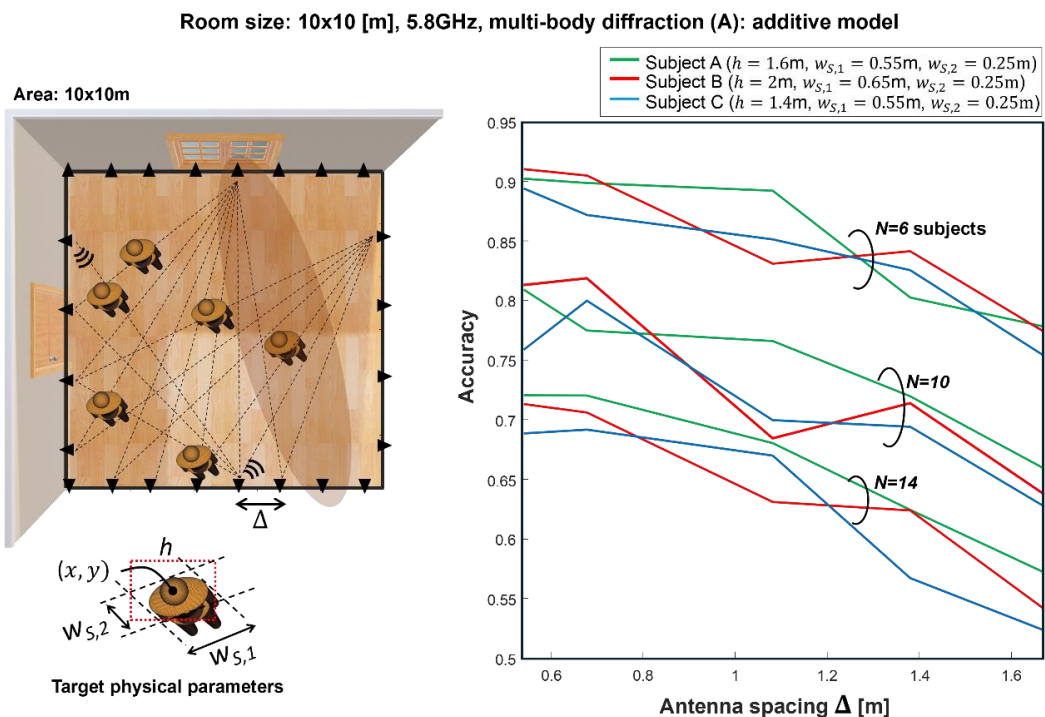


Figure 9: Accuracy analysis. Prediction of the number of subjects moving in a 10x10m area. Subjects A, B and C characterized by different physical characteristics (height  $h$ , lateral and anteroposterior dimensions  $w_{S,1}, w_{S,2}$ ). Accuracy is evaluated for varying antenna spacing  $\Delta$  [m] and 5.8GHz CSI data.

Accuracy analysis							
		Accuracy (Subject A)		Accuracy (Subject B)		Accuracy (Subject C)	
		60 antennas	25 antennas	60 antennas	25 antennas	60 antennas	25 antennas
<b>10x10 [m]</b>	<b>5.8GHz</b>	N = 3 subjects: 0.97	0.92	0.98	0.89	0.95	0.89
		N = 6 subjects: 0.90	0.78	0.90	0.77	0.87	0.75
		N = 10 subjects: 0.77	0.66	0.82	0.64	0.80	0.63
		N = 14 subjects: 0.72	0.57	0.71	0.54	0.69	0.52
		N = 20 subjects: 0.67	0.52	0.66	0.50	0.64	0.52
<b>10x10 [m]</b>	<b>2.4GHz</b>	N = 3 subjects: 0.97	0.91	0.99	0.94	0.99	0.88
		N = 6 subjects: 0.92	0.78	0.95	0.77	0.91	0.79
		N = 10 subjects: 0.82	0.65	0.86	0.69	0.83	0.65
		N = 14 subjects: 0.73	0.56	0.77	0.58	0.75	0.58
		N = 20 subjects: 0.69	0.55	0.69	0.55	0.72	0.52
		60 antennas	20 antennas	60 antennas	20 antennas	60 antennas	20 antennas
<b>7x7 [m]</b>	<b>5.8GHz</b>	N = 3 subjects: 0.97	0.89	0.98	0.89	0.98	0.90
		N = 6 subjects: 0.88	0.75	0.90	0.74	0.90	0.76
		N = 10 subjects: 0.70	0.61	0.80	0.61	0.79	0.62
		N = 14 subjects: 0.66	0.53	0.59	0.53	0.69	0.53
		N = 20 subjects: 0.59	0.49	0.48	0.50	0.58	0.50
<b>7x7 [m]</b>	<b>2.4GHz</b>	N = 3 subjects: 0.98	0.89	0.99	0.89	0.98	0.89
		N = 6 subjects: 0.92	0.78	0.89	0.74	0.92	0.78
		N = 10 subjects: 0.77	0.65	0.82	0.60	0.82	0.65
		N = 14 subjects: 0.71	0.57	0.70	0.54	0.73	0.59
		N = 20 subjects: 0.65	0.52	0.65	0.50	0.66	0.53
<b>5x5 [m]</b>	<b>5.8GHz</b>	N = 3 subjects: 0.95	0.94	0.98	0.93	0.96	0.93
		N = 6 subjects: 0.83	0.81	0.85	0.81	0.82	0.78
		N = 10 subjects: 0.69	0.66	0.66	0.66	0.72	0.69
		N = 14 subjects: 0.57	0.59	0.53	0.55	0.61	0.60
		N = 17 subjects: 0.53	0.58	0.51	0.56	0.62	0.57
<b>5x5 [m]</b>	<b>2.4GHz</b>	N = 3 subjects: 0.96	0.94	0.97	0.94	0.98	0.94
		N = 6 subjects: 0.88	0.85	0.89	0.82	0.87	0.82
		N = 10 subjects: 0.75	0.73	0.76	0.72	0.71	0.73
		N = 14 subjects: 0.64	0.61	0.65	0.64	0.69	0.61
		N = 17 subjects: 0.59	0.57	0.65	0.57	0.62	0.59

Figure 10: Accuracy analysis for varying area size ranging from 10m x 10m to 5m x 5m, and with CSI at 2.4GHz and 5.8 GHz. Subjects A, B and C characterized by different physical characteristics (height  $h$ , lateral and anteroposterior dimensions  $w_{S,1}, w_{S,2}$ ). Accuracy is obtained for varying number of antennas, namely 60 and 25 antennas for 10m x 10m area, 60 and 20 antennas for 5m x 5m and 7m x 7m area.

### 6.3. Multi-target discrimination: statistical parity

Considering the same deployment scenarios, we analyze now in detail the possibility of a performance disparity which might be observed among individuals with different physical sizes.

By defining as  $\hat{N}$  the estimated number of targets co-present in the same scene and  $P(\hat{N} = N|A)$  the probability of correctly identifying the true number of subjects  $N$  in the area, conditioned on

subjects characterized by physical characteristics (A), the statistical parity between a pair of subjects, i.e. type A and B, is defined, according to the discussion in the previous section, as

$$|p(\hat{N} = N|A) - p(\hat{N} = N|B)|$$

Notice that the larger the value the worse parity.

The table of Figure 12 reports a complete analysis of statistical parity considering the same cases of the table in Figure 10. A performance disparity is observed among individuals with different physical sizes, while such disparity generally increases with the number of subjects co-present. For example, the statistical parity exhibits a 4 to 5-fold increase upon scaling the number of targets from  $N=6$  to  $N=14$ . Although in many cases the optimization of the learning process keeps such disparity to a minimal value, there are still some cases (highlighted in red) where the recorded disparity is higher. Stronger equality (low disparity) comes at the cost of reduced accuracy: investigating such trade-off is still to be considered an open problem.

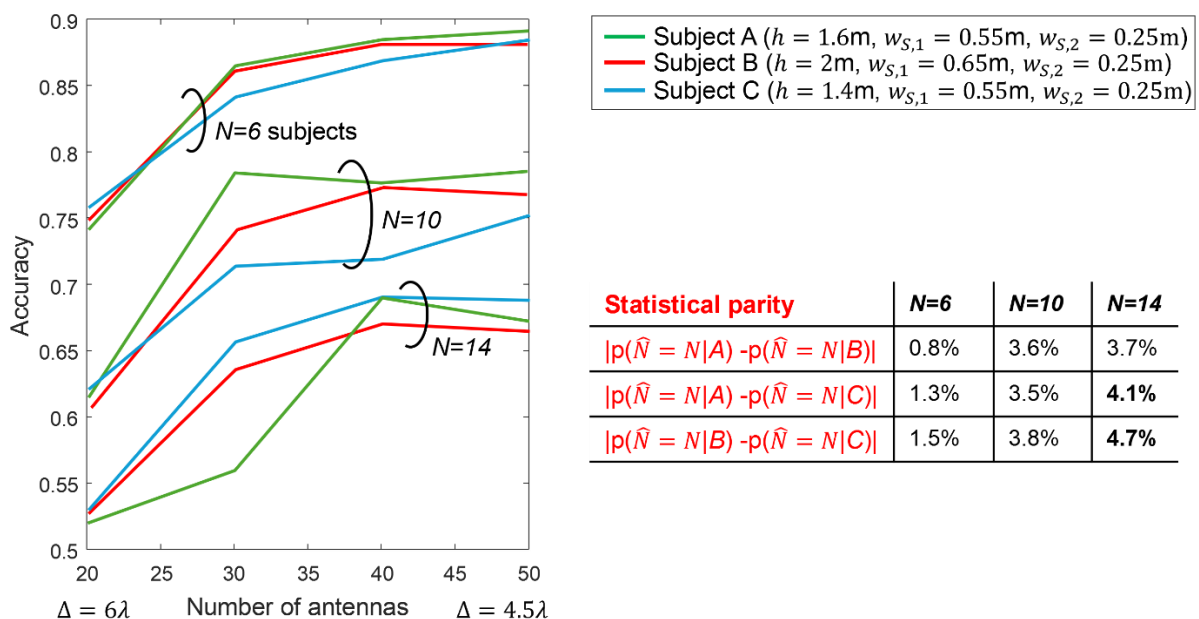


Figure 11: Accuracy and Statistical parity results. Prediction of the number of subjects moving in a 7x7m area. Subjects A, B and C characterized by different physical characteristics (height  $h$ , lateral and anteroposterior dimensions  $w_{S,1}, w_{S,2}$ ). Accuracy and statistical parity metrics obtained for varying antenna spacing  $\Delta$  [m] and simulated 5.8GHz CSI data.

### Statistical parity analysis

	$ \mathbf{p}(\hat{N} = N A) - \mathbf{p}(\hat{N} = N B) $	$ \mathbf{p}(\hat{N} = N A) - \mathbf{p}(\hat{N} = N C) $	$ \mathbf{p}(\hat{N} = N B) - \mathbf{p}(\hat{N} = N C) $
<b>10x10 [m] 5.8GHz</b>	N = 3 subjects: 0.015	<b>0.033</b>	<b>0.037</b>
	N = 6 subjects: <b>0.031</b>	0.016	0.020
	N = 10 subjects: 0.017	0.012	0.009
	N = 14 subjects: 0.015	0.016	0.019
	N = 20 subjects: 0.014	0.014	0.012
<b>10x10 [m] 2.4GHz</b>	N = 3 subjects: 0.015	0.016	0.024
	N = 6 subjects: 0.020	0.020	<b>0.025</b>
	N = 10 subjects: <b>0.023</b>	0.013	0.023
	N = 14 subjects: 0.016	0.015	0.012
	N = 20 subjects: 0.010	<b>0.030</b>	0.024
<b>7x7 [m] 5.8GHz</b>	N = 3 subjects: 0.008	0.008	0.010
	N = 6 subjects: 0.008	0.015	0.015
	N = 10 subjects: 0.036	<b>0.046</b>	0.036
	N = 14 subjects: 0.043	0.018	0.050
	N = 20 subjects: <b>0.082</b>	0.022	<b>0.073</b>
<b>7x7 [m] 2.4GHz</b>	N = 3 subjects: 0.013	0.004	0.014
	N = 6 subjects: 0.023	0.012	0.024
	N = 10 subjects: <b>0.064</b>	0.020	<b>0.045</b>
	N = 14 subjects: 0.017	0.017	0.021
	N = 20 subjects: 0.026	<b>0.059</b>	0.041
<b>5x5 [m] 5.8GHz</b>	N = 3 subjects: 0.012	0.014	0.005
	N = 6 subjects: 0.009	0.021	0.025
	N = 10 subjects: 0.029	0.025	0.025
	N = 14 subjects: <b>0.065</b>	<b>0.050</b>	<b>0.045</b>
	N = 20 subjects: 0.028	0.045	0.041
<b>5x5 [m] 2.4GHz</b>	N = 3 subjects: 0.007	0.013	0.008
	N = 6 subjects: 0.018	0.012	0.017
	N = 10 subjects: 0.025	0.023	0.027
	N = 14 subjects: <b>0.037</b>	<b>0.052</b>	0.028
	N = 20 subjects: 0.033	0.035	<b>0.032</b>

Figure 12: Statistical parity analysis for varying area size ranging from 10m x 10m to 5m x 5m, and with CSI at 2.4GHz and 5.8 GHz. Subjects A, B and C characterized by the same physical characteristics as in Figure 8. Statistical parity is computed for all combinations of targets, namely A v. B, A v. C and C v. B.

## 7. Conclusions

---

The deliverable explored the challenges and opportunities of ethics-by-design in RF sensing, examining both recent research and technological advancements in the field as well as possible risks and misuse of the technology. Emerging solutions to enable RF holography in dynamic environments are discussed together with data processing and hardware design choices to enable privacy by design. Ethical and privacy threats have been identified by focusing specifically on dynamic tracking of body movements. Next, the deliverable proposed and discussed three promising technical mitigation measures designed to limit the ability for unethical use of RF sensing technologies. These enablers target the problem of:

- 1) realizing a purpose-built EM environment, namely controlling the RF signal emissions or the manipulate the radio propagation by beam steering technology and reconfigurable EM surfaces
- 2) limiting personal data collection using physics-driven generative AI tools that effectively serve as “ethical filter” capable of generating depersonalized training data from a synthetic environment, enhance the transparency and scalability of RF sensing as well as its training data handling practices.
- 3) obtaining selective obfuscation via machine unlearning techniques which selectively unlearn functions that could potentially facilitate unethical use or unintended consequences

Ethical design models for RF sensing are finally discussed, exploring their potential role in future standardization and regulatory efforts.

### 3. References

---

- [1] P. M. Holl and F. Reinhard, "Holography of Wi-Fi radiation", *Phys. Rev. Lett.*, vol. 118, pp. 183901-May, 2017.
- [2] S. Savazzi, et al., "On the use of stray wireless signals for sensing: A look beyond 5G for the next generation of industry," *Computer*, vol. 52, no. 7, pp. 25-36, July 2019, doi: 10.1109/MC.2019.2913626.
- [3] B. Guo, et al. "Behavior recognition based on Wi-Fi CSI: Part 1 and 2", *IEEE Commun. Mag.*, vol. 55, no. 10, pp. 90, Oct. 2017.
- [4] R. Du *et al.*, "An Overview on IEEE 802.11bf: WLAN Sensing," *IEEE Communications Surveys & Tutorials*, to appear 2025. doi: 10.1109/COMST.2024.3408899
- [5] D. Avola, et al. "Person Re-Identification Through Wi-Fi Extracted Radio Biometric Signatures," *IEEE Transactions on Information Forensics and Security*, vol. 17, pp. 1145-1158, 2022
- [6] F. Paonessa, G. Virone, S. Kianoush, A. Nordio and S. Savazzi, "An Initial Study of Human-Scale Blockage in sub-THz Radio Propagation with Application to Indoor Passive Localization," *2024 IEEE-APS Topical Conference on Antennas and Propagation in Wireless Communications (APWC)*, Lisbon, Portugal, 2024, pp. 50-54, doi: 10.1109/APWC61918.2024.10701955.
- [7] J. -F. Determe, et al., "Monitoring Large Crowds With WiFi: A Privacy-Preserving Approach," *IEEE Systems Journal*, vol. 16, no. 2, pp. 2148-2159, June 2022
- [8] S. Palipana, et al. "Pantomime: Mid-air gesture recognition with sparse millimeter-wave radar point clouds." *Proceedings of the ACM on interactive, mobile, wearable and ubiquitous technologies*, vol 5 no. 1 pp.1-27, 2021.
- [9] H. Liu et al., "Real-time Arm Gesture Recognition in Smart Home Scenarios via Millimeter Wave Sensing," *Proc. ACM Interact. Mob. Wearable Ubiquitous Technol.*, 28 pp, Dec. 2020.
- [10] S. Savazzi, et al., "Electromagnetic-informed generative models for passive RF sensing and perception of body motions," *IEEE Open J. of Ant. and Prop.*, vol. 5, no. 4, pp. 958-973, Aug. 2024.
- [11] F. Meneghello, et al., "A CSI Dataset for Wireless Human Sensing on 80 MHz Wi-Fi Channels," *IEEE Communications Magazine*, vol. 61, no. 9, pp. 146-152, September 2023.
- [12] P. S. Thomas et al. "Preventing undesirable behavior of intelligent machines," *Science*, Nov. 2019
- [13] Jie Xu, et al. "Machine Unlearning: Solutions and Challenges", *IEEE Transactions on Emerging Topics in Computational Intelligence*, vol.8, no.3, pp.2150-2168, 2024.
- [14] Swierstra, T., Stemmerding, D., Boenink, M. (2009). Exploring Techno-Moral Change: The Case of the Obesity Pill. In: Sollie, P., Düwell, M. (eds) *Evaluating New Technologies. The International Library of Ethics, Law and Technology*, vol 3. Springer, Dordrecht. [https://doi.org/10.1007/978-90-481-2229-5\\_9](https://doi.org/10.1007/978-90-481-2229-5_9)
- [15] L. Bariah, et al. "Large Generative AI Models for Telecom: The Next Big Thing?," *IEEE Commun. Mag.*, to appear, 2024.

- [16] Palumbo, et al. "Objective metrics for ethical AI: a systematic literature review," *Int J Data Sci Anal*, 2024.
- [17] S. Kianoush, et al. "Joint RIS-Assisted Localization and Communication: A Tradeoff Among Accuracy, Spectrum Efficiency, and Time Resource," *IEEE Sensors Journal*, vol. 25, no. 3, pp. 5630-5643, 1 Feb.1, 2025,
- [18] S. Cammers-Goodwin, N. Gertz, C. Ayding, "Moralizing Radio Frequency (RF) Photography using Techno-moral Scenarios" *Proc. of IEEE International Conference on Emerging Technologies and Factory Automation*, September 2024, Padova, Italy
- [19] Duvenaud, D. K.; Maclaurin, D.; Iparraguirre, J.; Bombarell, R.; Hirzel, T.; Aspuru-Guzik, A.; and Adams, R. P. 2015. Convolutional networks on graphs for learning molecular fingerprints. In *Advances in neural information processing systems*, 2224--2232.
- [20] Lei, T.; Jin,W.; Barzilay, R.; and Jaakkola, T. 2017. Deriving neural architectures from sequence and graph kernels. In *Precup, D., and Teh, Y.W., eds., Proceedings of the 34th International Conference on Machine Learning*, volume 70 of *Proceedings of Machine Learning Research*, 2024--2033. International Convention Centre, Sydney, Australia: PMLR.
- [21] Stefano Savazzi. (2024). WiFi frame datasets for body motion discrimination [Data set]. Kaggle, [Online] Available: <https://doi.org/10.34740/KAGGLE/DS/4802891>.
- [22] C. Guo, G. Pleiss, Y. Sun, and K. Q. Weinberger, "On calibration of modern neural networks," 2017. [Online]. Available: <https://arxiv.org/abs/1706.04599>
- [23] S. Kianoush et al., "Advancing Passive Localization via Beamsteering in Near-Field ISAC Systems" *Proc. of IEEE Workshop of Statistical Processing*, to appear 2025.
- [24] U. Milasheuski et al. "Bayesian Federated Learning for Continual Training" *Proc. IEEE Workshop of Statistical Processing, Proc. of IEEE Workshop of Statistical Signal Processing*, to appear 2025.

## 9. List of figures

---

Figure 1: RF holography system to repurpose communication networks: architecture example, CSI reports and analytics.....	10
Figure 2: Holographic imaging: body scanning concept for a human phantom .....	12
Figure 3: Smart and reconfigurable radio environment example: beam-switched system integrated with WiFi setups, reconfigurable and smart skin antenna surfaces.....	15
Figure 4: Physics-driven generative machine learning example for reproduction of the array response from a ULA of 9 antennas. Ethical filtering for depersonalized training data.....	17
Figure 5: Localization of mobile device (UEs) inside a confined region using active RIS components: the smart radio environment is simulated for communication performance assessment: two UE are moving randomly in the monitored area and communicating with the BS.....	19
Figure 6: Root Mean Square Error (RMSE) result of UE localization Using CNN and vision transformers (ViT) for the same scenario presented in figure 7. The RMSE result for $N_{sym}=250$ (i.e., simulated samples) and for varying number of RIS electronic rotations $R$ .....	20
Figure 7: Infrastructure snapshot scenario: multi-target body counting through RF signals inspection. EM simulation environment, main parameters, network structure and DGCNN model approach.....	23
Figure 8: Infrastructure snapshot scenario: deployment and tests in an indoor environment. Results will be discussed in WP6 .....	24
Figure 9: Accuracy analysis. Prediction of the number of subjects moving in a 10x10m area. Subjects A, B and C characterized by different physical characteristics (height $h$ , lateral and anteroposterior dimensions $wS, 1, wS, 2$ ). Accuracy is evaluated for varying antenna spacing $\Delta$ [m] and 5.8GHz CSI data.....	26
Figure 10: Accuracy analysis for varying area size ranging from 10m x 10m to 5m x 5m, and with CSI at 2.4GHz and 5.8 GHz. Subjects A, B and C characterized by different physical characteristics (height $h$ , lateral and anteroposterior dimensions $wS, 1, wS, 2$ ). Accuracy is obtained for varying number of antennas, namely 60 and 25 antennas for 10m x 10m area, 60 and 20 antennas for 5m x 5m and 7m x 7m area. ....	27
Figure 11: Accuracy and Statistical parity results. Prediction of the number of subjects moving in a 7x7m area. Subjects A, B and C characterized by different physical characteristics (height $h$ , lateral and anteroposterior dimensions $wS, 1, wS, 2$ ). Accuracy and statistical parity metrics obtained for varying antenna spacing $\Delta$ [m] and simulated 5.8GHz CSI data.....	28
Figure 12: Statistical parity analysis for varying area size ranging from 10m x 10m to 5m x 5m, and with CSI at 2.4GHz and 5.8 GHz. Subjects A, B and C characterized by the same physical characteristics as in Figure 8. Statistical parity is computed for all combinations of targets, namely A v. B, A v. C and C v. B. ....	29